sRAKI-RNN: Accelerated MRI with Scan-Specific Recurrent Neural Networks using Densely Connected Blocks

Seyed Amir Hossein Hosseini[a, b], Chi Zhang[a, b], Kâmil Uğurbil[b], Steen Moeller[b], and Mehmet Akçakaya[a, b]

[a]Electrical and Computer Engineering, University of Minnesota, Minneapolis, MN, USA
[b]Center for Magnetic Resonance Research, University of Minnesota, Minneapolis, MN, USA

ABSTRACT

This study aims to improve upon Self-consistent Robust Artificial-neural-networks for k-space Interpolation (sRAKI), which is a deep learning-based parallel imaging technique for accelerated MRI reconstruction. The proposed technique, called sRAKI-RNN, combines the calibration and reconstruction phases of sRAKI into a single step that jointly learns the self-consistency rule and performs iterative reconstruction using recurrent neural networks (RNN). Similar to sRAKI, sRAKI-RNN supports arbitrary undersampling patterns and is a database-free technique that is trained on autocalibrating signal (ACS) data from the same scan. Densely connected blocks are used in each iteration of the RNN to improve the convergence during the learning phase. sRAKI-RNN was evaluated on targeted right coronary artery (RCA) MRI. The results indicate that sRAKI-RNN further improves the noise resilience of sRAKI in a shorter running time and also considerably outperforms its linear counterpart, SPIRiT, in suppressing reconstruction noise.

Keywords: Accelerated MRI, parallel imaging, coronary MRI, deep learning, recurrent neural networks, dense neural networks

1. INTRODUCTION

Coronary MRI provides a non-invasive and radiation-free tool in diagnosis of coronary artery disease (CAD),[1] the leading cause of death in the United States.[2] Coronary MRI is typically acquired with electrocardiogram (ECG) triggering during diastolic quiescence and in free-breathing, leading to long scan durations and necessitating accelerated imaging.[3–5] Parallel imaging,[6,7] compressed sensing[8–10] and their combinations[11–17] are some of the methods that have been used for accelerated coronary MRI. Recently, numerous research studies have focused on deep learning-based techniques for accelerated MRI in general.[18–29] These techniques mostly depend on large databases of fully-sampled datasets for training neural networks that perform nonlinear end-to-end mapping from undersampled data to fully-sampled target data. However, in some MRI applications such as whole heart coronary MRI,[30–32] reference fully-sampled data cannot be acquired due to impractically long scan times. Robust artificial-neural-networks for k-space interpolation (RAKI)[18] is a machine learning-based technique, which trains convolutional neural networks (CNN) on scan-specific autocalibrating signal (ACS) data, and thus addresses this issue. This scan-specificity feature of RAKI also ensures that inter-scan or inter-individual variability of training data does not adversely affect the generalizability of learning for reconstruction.[33]

RAKI, which was originally designed for uniform undersampling, has been recently extended with an approach called self-consistent RAKI (sRAKI) to support arbitrary undersampling patterns for applications that benefit from random undersampling such as coronary MRI.[34–36] The notion of self-consistency in sRAKI is similar to that proposed in SPIRiT.[37] However, in sRAKI, a nonlinear mapping using CNNs is learnt as the self-consistency rule instead of the linear convolutions in SPIRiT. Similar to SPIRiT, sRAKI also performs the calibration and reconstruction in separate phases, which can degrade efficiency of reconstruction. In this study, we sought to combine these two steps by using recurrent neural networks (RNN)[23,24,26,38] with multiple densely connected neural network blocks.[39] The new technique, called sRAKI-RNN is evaluated in coronary MRI and compared to SPIRiT and sRAKI for various acceleration rates.

Further author information: (Send correspondence to M.A.)
M.A.: E-mail: akcakaya@umn.edu, Telephone: +1 612 625 1343
S.A.H.: E-mail: hosse049@umn.edu

2. MATERIALS AND METHODS

Let $\mathbf{x}$ denote the full k-space data across all coils and $\mathbf{y}$ be the corresponding acquired undersampled noisy data from a multi-coil MRI system with n_c coils. The forward model for this system is formulated as:

$$\mathbf{y} = \mathbf{D}\mathbf{x} + \mathbf{n}, \tag{1}$$

where $\mathbf{D}$ is the undersampling operator and $\mathbf{n}$ represents acquisition noise. The following objective function is optimized to estimate the full k-space data $\mathbf{x}$ from measurements $\mathbf{y}$ by using the self-consistency notion of SPIRiT:[37]

$$\arg\min_{\mathbf{x}} \|\mathbf{y} - \mathbf{D}\mathbf{x}\|_2^2 + \beta\|\mathbf{x} - \mathbf{G}(\mathbf{x})\|_2^2, \tag{2}$$

where $\mathbf{G}(\cdot)$ represents the self-consistency interpolation function. The first term in objective function (2) ensures that the reconstructed data remains consistent with the acquired portion of data. The second term enforces the self-consistency rule of $\mathbf{G}(\cdot)$ on the reconstructed data and β is a weight term. SPIRiT assumes a linear self-consistency rule,[37] whereas sRAKI generalizes the interpolating function $\mathbf{G}(\cdot)$ to a nonlinear mapping that can be learned by CNNs.[34–36] In both approaches, the self-consistency rule is determined by training on ACS data prior to reconstruction. Subsequently, the objective function in (2) can be optimized iteratively by alternating between enforcing data consistency and self-consistency.[37]

An alternative approach is to unroll iterations in an RNN[23,24,26,38] with multiple CNN blocks each implementing the unrolled version of this iterative approach. For the n^{th} unrolled iteration, the self-consistency and data-consistency operations are applied as follows:

$$\begin{cases} \mathbf{z}_n = \mathbf{G}(\mathbf{x}_n), \\ \mathbf{x}_{n+1} = (\mathbf{I} - \mathbf{D}^T\mathbf{D})\mathbf{z}_n + \mathbf{D}^T\mathbf{y}, \end{cases} \tag{3}$$

where $\mathbf{x}_n$ is the reconstructed k-space data at iteration n, $\mathbf{z}_n$ is the output of self-consistency unit and $\mathbf{I}$ is the identity operator. Thus, the second equation in (3) enforces data-consistency with acquired data $\mathbf{y}$. This approach, called sRAKI-RNN, eliminates the need for a separate calibration of CNNs in sRAKI to specify the self-consistency rule $\mathbf{G}(\cdot)$. Instead, sRAKI-RNN trains an end-to-end network to concurrently learn the self-consistency rule and implement the iterative scheme of reconstruction in sRAKI. Hence, the reconstruction phase of sRAKI-RNN is a single forward propagation step in training neural networks . In addition, since the CNN parameters are shared across iterations, the training phase can be efficiently performed using the ACS data, as in sRAKI, maintaining scan-specificity.

2.1 Implementation Details

In this study, an RNN architecture unrolled for 5 iterations was employed to perform an end-to-end k-space reconstruction (Figure 1). Each iteration consists of a single self-consistency (SC) and data-consistency (DC) unit, connected to each other. For the self-consistency unit, 3 blocks of densely connected CNNs[39] followed by a single convolutional layer were employed with 2 outer skip connections (see Figure 1) to further facilitate the flow of information across blocks. Each dense block (DB) consisted of 3 convolutional layers with a growth factor of 8 channels. All layers in the dense blocks were followed by rectifier linear units (ReLU) as activation functions. The kernel size of all convolutional layers was 3×3.

To generate training data, ACS region was retrospectively undersampled in $k_y - k_z$ plane using a single Poisson-disc pattern with a rate identical to the rest of data. The undersampled and full ACS data pairs were later used to train the network. To reduce the training computational complexity, 3D data were first inverse-Fourier transformed along readout direction, k_x. The resultant 2D slices were then fed to the network in batch sizes of 32. The real and imaginary components of complex k-space data were concatenated before feeding them into the network, which led to $2n_c$ input and output channels. The network was trained by minimizing an MSE loss function using Adam optimizer with a learning rate of 0.001, iterated over 500 epochs. To standardize the hyper-parameters such as the learning rate, the k-space was scaled such that the maximum absolute value was 1. For comparison purposes, SPIRiT using a conjugate gradient reconstruction[37] and sRAKI with the parameters as previously described[34–36] were also implemented.

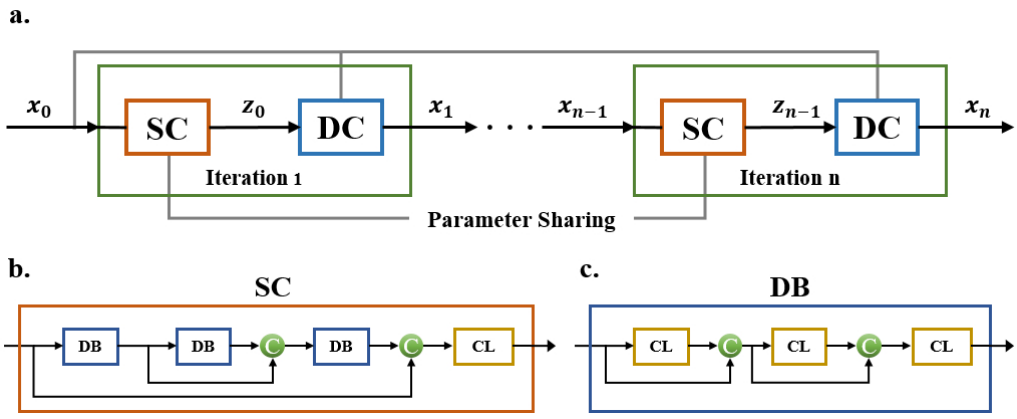

Figure 1. (a) The recurrent network architecture of sRAKI-RNN unrolled for n iterations to simultaneously apply self-consistency (SC) and data consistency (DC) and perform the iterative reconstruction. (b) A single SC unit with 3 dense blocks (DB), a single convolutional layer (CL) at the output, along with two skip connections to facilitate information flow through network. (c) A closer view of the DB.

2.2 In Vivo Coronary MRI

Targeted right coronary artery (RCA) MRI was acquired on a 28-year old male subject using a 3T Siemens Magnetom Prisma (Siemens Healthineers, Erlangen, Germany) system with a 30-channel receiver body coil-array and an ECG-triggered GRE sequence with imaging parameters: TR/TE=3.4/1.5ms, flip angle=20°, bandwidth=601 Hz/pixel, field-of-view (FOV)=300 × 300 × 48mm^3, resolution=1 × 1 × 3mm^3, navigator window=5mm. T_2-preparation and a spectrally-selective fat saturation were utilized for improved contrast. The 3D k-space data was exported and retrospectively undersampled with a Poisson disc pattern at acceleration rates 2, 3, 4, and 5 with a fully-sampled 36 × 10 ACS region in $k_y - k_z$ plane. The images reconstructed using SPIRiT, sRAKI and sRAKI-RNN were quantitatively assessed by normalized mean square error (NMSE) and structural similarity index (SSIM) metrics with respect to the reference fully-sampled image. Final images were obtained using root sum-squares combination of all coil images. All algorithms were implemented in Python, and processed on a workstation with an Intel E5-2640V3 CPU (2.6GHz and 256GB memory), and an NVIDIA Tesla V100 GPU with 32GB memory.

3. RESULTS

Figure 2 depicts a representative slice from the targeted RCA MRI dataset that was retrospectively undersampled at rates 2, 3, 4 and 5, and reconstructed using techniques SPIRiT, sRAKI and sRAKI-RNN. All techniques successfully remove aliasing artifacts and allow visualization of the RCA at all rates. Nonetheless, reconstruction noise is amplified by SPIRiT, especially at higher rates. Both sRAKI and sRAKI-RNN demonstrate desirable noise properties, with sRAKI-RNN being superior in suppressing reconstruction noise at all rates.

A quantitative analysis is provided in Table 1 for the NMSE and SSIM metrics. These values, which are consistent with the visual evaluation of Figure 2, further indicate that sRAKI-RNN improves accelerated coronary MRI reconstruction over SPIRiT and sRAKI.

4. DISCUSSION

We proposed an accelerated MRI reconstruction technique, sRAKI-RNN that uses an RNN with densely connected blocks to enforce self-consistency among multi-coil MRI datasets and data-consistency with arbitrarily undersampled data. sRAKI-RNN further improves the desirable noise properties of our previous technique, sRAKI.[34–36] In contrast to most deep learning-based accelerated MRI reconstruction methods that need large amounts of data to train neural networks,[19–29] sRAKI-RNN inherits the scan-specificity feature of the RAKI and sRAKI methods. Consequently, sRAKI-RNN relies on ACS data from the same scan to train the neural

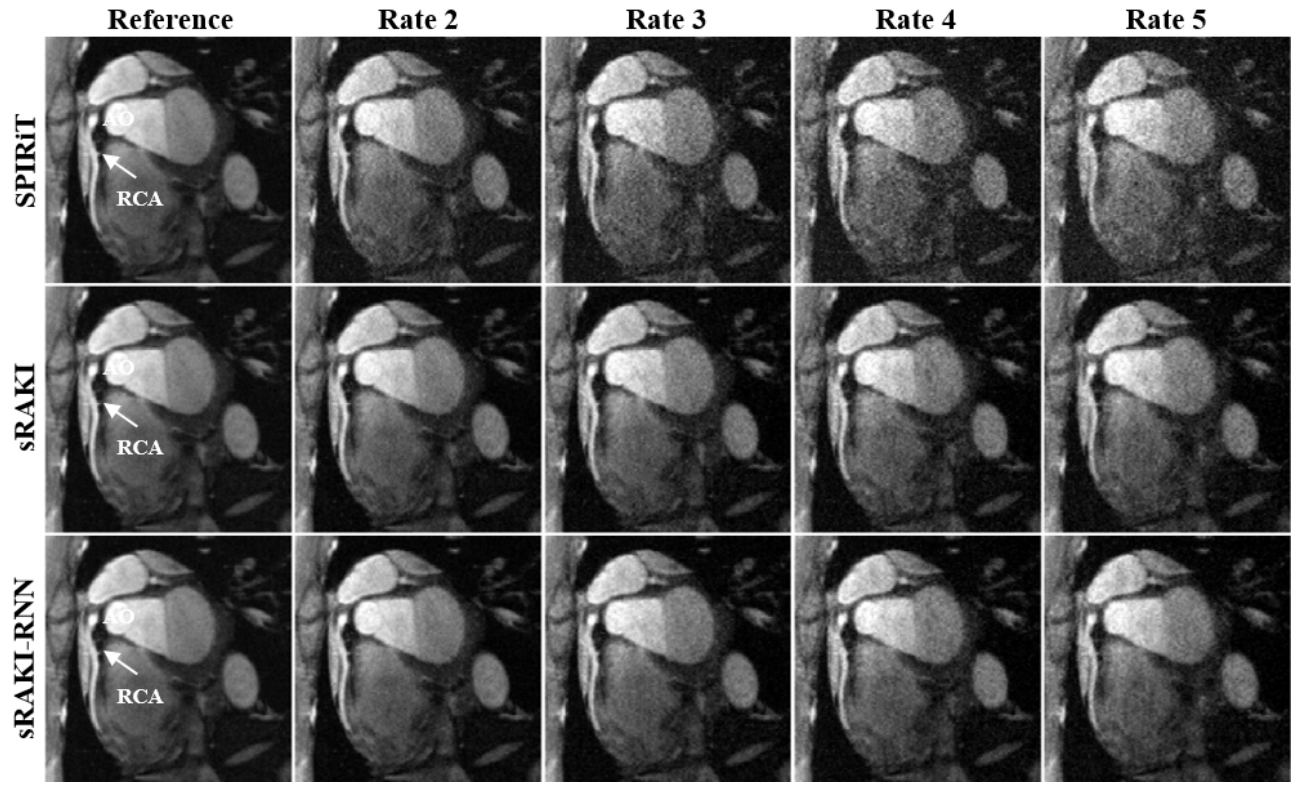

Figure 2. A representative slice from a 3D right coronary artery MRI data of a healthy subject. The data were retrospectively undersampled at rates 2, 3, 4 and 5 in the $k_y - k_z$ plane and then reconstructed using techniques SPIRiT, sRAKI and sRAKI-RNN (top, middle and bottom rows). The fully-sampled images are provided in the first column as a reference for comparison. All techniques successfully remove aliasing artifacts, and the least reconstruction noise is achieved by sRAKI-RNN. (RCA: right coronary artery; AO: aortic root)

network, which is particularly beneficial for applications where long scans impede acquiring fully-sampled data, such as whole-heart imaging.[30–32]

By using an unrolled RNN scheme with parameter sharing across iterations, sRAKI-RNN combines the calibration and reconstruction phases of sRAKI into a single training phase. This compaction reduced the total running time of sRAKI-RNN to approximately 60 seconds, which is twice faster than sRAKI. In addition, fewer hyper-parameters (e.g. learning rate of gradient descent) are involved in the whole reconstruction process, which further facilitates training. Another difference with sRAKI is that sRAKI-RNN utilizes a densely connected neural network design for the self-consistency units. This configuration with outer skip connections considerably improved convergence of training by facilitating the flow of information across blocks. We note that such a

Table 1. Quantitative NMSE (left) and SSIM (right) assessment of SPIRiT, sRAKI and sRAKI-RNN in reconstructing a right coronary artery MRI dataset at acceleration rates 2, 3, 4 and 5. sRAKI-RNN achieves the least NMSE and the highest SSIM values at all rates.

NMSE	R2	R3	R4	R5
SPIRiT	0.0119	0.0205	0.0334	0.0449
sRAKI	0.0090	0.0162	0.0215	0.0253
sRAKI-RNN	0.0079	0.0145	0.0197	0.0238

SSIM	R2	R3	R4	R5
SPIRiT	0.907	0.855	0.792	0.748
sRAKI	0.945	0.906	0.875	0.853
sRAKI-RNN	0.954	0.919	0.893	0.874

design for sRAKI leads the network to learn a trivial identity mapping for the self-consistency rule due to the skip connections, since input and target data are identical in calibration phase of sRAKI.

We have compared the performance of sRAKI-RNN with SPIRiT and sRAKI in a targeted RCA dataset. Visual and quantitative evaluation of the results indicate that sRAKI-RNN considerably reduces amplification of reconstruction noise in SPIRiT, particularly at higher acceleration rates. In addition, sRAKI-RNN improves noise properties of sRAKI at all acceleration rates.

5. CONCLUSION

sRAKI-RNN is a deep learning-based accelerated MRI technique that supports reconstruction with arbitrary undersampling patterns. It uses an unrolled RNN approach with parameter sharing across iterations besides the densely connected configuration of units used to learn the k-space self-consistency rule of multi-coil MRI dataset. Furthermore, these networks are trained on scan-specific calibration data without requiring large amounts of data. sRAKI-RNN outperforms SPIRiT and sRAKI in suppressing reconstruction noise with a shorter running time.

ACKNOWLEDGMENTS

This work was supported by NIH, Grant numbers: R00HL111410, P41EB015894, U01EB025144, P41EB027061; NSF, Grant number: CAREER CCF-1651825

REFERENCES

[1] Kim, W. Y., Danias, P. G., Stuber, M., Flamm, S. D., Plein, S., Nagel, E., Langerak, S. E., Weber, O. M., Pedersen, E. M., Schmidt, M., et al., "Coronary magnetic resonance angiography for the detection of coronary stenoses," *New England Journal of Medicine* **345**(26), 1863–1869 (2001).

[2] Benjamin, E. J., Muntner, P., and Bittencourt, M. S., "Heart disease and stroke statistics-2019 update: a report from the american heart association," *Circulation* **139**(10), e56–e528 (2019).

[3] Stuber, M., Botnar, R. M., Danias, P. G., Sodickson, D. K., Kissinger, K. V., Van Cauteren, M., De Becker, J., and Manning, W. J., "Double-oblique free-breathing high resolution three-dimensional coronary magnetic resonance angiography," *Journal of the American College of Cardiology* **34**(2), 524–531 (1999).

[4] Oshinski, J. N., Hofland, L., Mukundan J., S., Dixon, W. T., Parks, W. J., and Pettigrew, R. I., "Two-dimensional coronary MR angiography without breath holding.," *Radiology* **201**(3), 737–743 (1996).

[5] McConnell, M. V., Khasgiwala, V. C., Savord, B. J., Chen, M. H., Chuang, M. L., Manning, W. J., and Edelman, R. R., "Prospective adaptive navigator correction for breath-hold MR coronary angiography," *Magnetic Resonance in Medicine* **37**(1), 148–152 (1997).

[6] Hu, P., Chan, J., Ngo, L. H., Smink, J., Goddu, B., Kissinger, K. V., Goepfert, L., Hauser, T. H., Rofsky, N. M., Manning, W. J., et al., "Contrast-enhanced whole-heart coronary MRI with bolus infusion of gadobenate dimeglumine at 1.5 T," *Magnetic Resonance in Medicine* **65**(2), 392–398 (2011).

[7] Bi, X., Carr, J. C., and Li, D., "Whole-heart coronary magnetic resonance angiography at 3 tesla in 5 minutes with slow infusion of gd-bopta, a high-relaxivity clinical contrast agent," *Magnetic Resonance in Medicine: An Official Journal of the International Society for Magnetic Resonance in Medicine* **58**(1), 1–7 (2007).

[8] Akçakaya, M., Basha, T. A., Chan, R. H., Rayatzadeh, H., Kissinger, K. V., Goddu, B., Goepfert, L. A., Manning, W. J., and Nezafat, R., "Accelerated contrast-enhanced whole-heart coronary MRI using low-dimensional-structure self-learning and thresholding," *Magnetic resonance in medicine* **67**(5), 1434–1443 (2012).

[9] Feng, L., Coppo, S., Piccini, D., Yerly, J., Lim, R. P., Masci, P. G., Stuber, M., Sodickson, D. K., and Otazo, R., "5D whole-heart sparse MRI," *Magnetic Resonance in Medicine* **79**(2), 826–838 (2018).

[10] Akçakaya, M., Basha, T. A., Goddu, B., Goepfert, L. A., Kissinger, K. V., Tarokh, V., Manning, W. J., and Nezafat, R., "Low-dimensional-structure self-learning and thresholding: regularization beyond compressed sensing for MRI reconstruction," *Magnetic Resonance in Medicine* **66**(3), 756–767 (2011).

[11] Akçakaya, M., Basha, T. A., Chan, R. H., Manning, W. J., and Nezafat, R., "Accelerated isotropic sub-millimeter whole-heart coronary MRI: compressed sensing versus parallel imaging," *Magnetic Resonance in Medicine* **71**(2), 815–822 (2014).

[12] Piccini, D., Feng, L., Bonanno, G., Coppo, S., Yerly, J., Lim, R. P., Schwitter, J., Sodickson, D. K., Otazo, R., and Stuber, M., "Four-dimensional respiratory motion-resolved whole heart coronary MR angiography," *Magnetic Resonance in Medicine* **77**(4), 1473–1484 (2017).

[13] Forman, C., Piccini, D., Grimm, R., Hutter, J., Hornegger, J., and Zenge, M. O., "High-resolution 3D whole-heart coronary MRA: a study on the combination of data acquisition in multiple breath-holds and 1D residual respiratory motion compensation," *Magnetic Resonance Materials in Physics, Biology and Medicine* **27**(5), 435–443 (2014).

[14] Correia, T., Ginami, G., Cruz, G., Neji, R., Rashid, I., Botnar, R. M., and Prieto, C., "Optimized respiratory-resolved motion-compensated 3 DC artesian coronary MR angiography," *Magnetic Resonance in Medicine* **80**(6), 2618–2629 (2018).

[15] Aitken, A. P., Henningsson, M., Botnar, R. M., Schaeffter, T., and Prieto, C., "100% efficient three-dimensional coronary MR angiography with two-dimensional beat-to-beat translational and bin-to-bin affine motion correction," *Magnetic Resonance in Medicine* **74**(3), 756–764 (2015).

[16] Cruz, G., Atkinson, D., Henningsson, M., Botnar, R. M., and Prieto, C., "Highly efficient nonrigid motion-corrected 3D whole-heart coronary vessel wall imaging," *Magnetic Resonance in Medicine* **77**(5), 1894–1908 (2017).

[17] Munoz, C., Cruz, G., Neji, R., Botnar, R. M., and Prieto, C., "Motion corrected water/fat whole-heart coronary MR angiography with 100% respiratory efficiency," *Magnetic Resonance in Medicine* **82**(2), 732–742 (2019).

[18] Akçakaya, M., Moeller, S., Weingärtner, S., and Uğurbil, K., "Scan-specific robust artificial-neural-networks for k-space interpolation (RAKI) reconstruction: Database-free deep learning for fast imaging," *Magnetic Resonance in Medicine* **81**(1), 439–453 (2019).

[19] Wang, S., Su, Z., Ying, L., Peng, X., Zhu, S., Liang, F., Feng, D., and Liang, D., "Accelerating magnetic resonance imaging via deep learning," in [*2016 IEEE 13th International Symposium on Biomedical Imaging (ISBI)*], 514–517, IEEE (2016).

[20] Hammernik, K., Klatzer, T., Kobler, E., Recht, M. P., Sodickson, D. K., Pock, T., and Knoll, F., "Learning a variational network for reconstruction of accelerated MRI data," *Magnetic Resonance in Medicine* **79**(6), 3055–3071 (2018).

[21] Lee, D., Yoo, J., Tak, S., and Ye, J. C., "Deep residual learning for accelerated MRI using magnitude and phase networks," *IEEE Transactions on Biomedical Engineering* **65**(9), 1985–1995 (2018).

[22] Han, Y., Yoo, J., Kim, H. H., Shin, H. J., Sung, K., and Ye, J. C., "Deep learning with domain adaptation for accelerated projection-reconstruction MR," *Magnetic Resonance in Medicine* **80**(3), 1189–1205 (2018).

[23] Aggarwal, H. K., Mani, M. P., and Jacob, M., "Modl: Model-based deep learning architecture for inverse problems," *IEEE Transactions on Medical Imaging* **38**(2), 394–405 (2018).

[24] Qin, C., Schlemper, J., Caballero, J., Price, A. N., Hajnal, J. V., and Rueckert, D., "Convolutional recurrent neural networks for dynamic MR image reconstruction," *IEEE Transactions on Medical Imaging* **38**(1), 280–290 (2018).

[25] Kwon, K., Kim, D., and Park, H., "A parallel MR imaging method using multilayer perceptron," *Medical Physics* **44**(12), 6209–6224 (2017).

[26] Schlemper, J., Caballero, J., Hajnal, J. V., Price, A. N., and Rueckert, D., "A deep cascade of convolutional neural networks for dynamic MR image reconstruction," *IEEE Transactions on Medical Imaging* **37**(2), 491–503 (2017).

[27] Yang, G., Yu, S., Dong, H., Slabaugh, G., Dragotti, P. L., Ye, X., Liu, F., Arridge, S., Keegan, J., Guo, Y., et al., "Dagan: deep de-aliasing generative adversarial networks for fast compressed sensing MRI reconstruction," *IEEE Transactions on Medical Imaging* **37**(6), 1310–1321 (2017).

[28] Hyun, C. M., Kim, H. P., Lee, S. M., Lee, S., and Seo, J. K., "Deep learning for undersampled MRI reconstruction," *Physics in Medicine & Biology* **63**(13), 135007 (2018).

[29] Eo, T., Jun, Y., Kim, T., Jang, J., Lee, H., and Hwang, D., "KIKI-net: cross-domain convolutional neural networks for reconstructing undersampled magnetic resonance images," *Magnetic Resonance in Medicine* **80**(5), 2188–2201 (2018).

[30] Niendorf, T., Hardy, C. J., Giaquinto, R. O., Gross, P., Cline, H. E., Zhu, Y., Kenwood, G., Cohen, S., Grant, A. K., Joshi, S., et al., "Toward single breath-hold whole-heart coverage coronary MRA using highly accelerated parallel imaging with a 32-channel MR system," *Magnetic Resonance in Medicine: An Official Journal of the International Society for Magnetic Resonance in Medicine* **56**(1), 167–176 (2006).

[31] Weber, O. M., Martin, A. J., and Higgins, C. B., "Whole-heart steady-state free precession coronary artery magnetic resonance angiography," *Magnetic Resonance in Medicine: An Official Journal of the International Society for Magnetic Resonance in Medicine* **50**(6), 1223–1228 (2003).

[32] Etienne, A., Botnar, R. M., Van Muiswinkel, A., Boesiger, P., Manning, W. J., and Stuber, M., "soap-bubble visualization and quantitative analysis of 3D coronary magnetic resonance angiograms," *Magnetic Resonance in Medicine: An Official Journal of the International Society for Magnetic Resonance in Medicine* **48**(4), 658–666 (2002).

[33] Eldar, Y. C., Hero III, A. O., Deng, L., Fessler, J., Kovacevic, J., Poor, H. V., and Young, S., "Challenges and open problems in signal processing: Panel discussion summary from ICASSP 2017 [panel and forum]," *IEEE Signal Processing Magazine* **34**(6), 8–23 (2017).

[34] Hosseini, S. A. H., Moeller, S., Weingartner, S., Ugurbil, K., and Akcakaya, M., "Accelerated coronary MRI using 3D SPIRiT-RAKI with sparsity regularization," *Proc. IEEE International Symposium on Biomedical Imaging* (2019).

[35] Hosseini, S. A. H., Moeller, S., Weingartner, S., Ugurbil, K., and Akcakaya, M., "Accelerated coronary MRI using SPIRiT-RAKI with gradient descent-based self-consistency," SCMR 22nd Annual Scientific Sessions (February 2019).

[36] Hosseini, S. A. H., Moeller, S., Weingartner, S., Ugurbil, K., and Akcakaya, M., "Accelerated targeted coronary MRI using sparsity-regularized SPIRiT-RAKI," ISMRM 27th Annual Meeting and Exhibition (May 2019).

[37] Lustig, M. and Pauly, J. M., "SPIRiT: Iterative self–consistent parallel imaging reconstruction for arbitrary k-space," *Magnetic Resonance in Medicine* **64**, 457–471 (2010).

[38] Zhang, K., Zuo, W., Gu, S., and Zhang, L., "Learning deep CNN denoiser prior for image restoration," in [*Proceedings of the IEEE Conference on Computer Vision and Pattern Recognition*], 3929–3938 (2017).

[39] Huang, G., Liu, Z., Van Der Maaten, L., and Weinberger, K. Q., "Densely connected convolutional networks," in [*Proceedings of the IEEE Conference on Computer Vision and Pattern Recognition*], 4700–4708 (2017).